Synthesis of Mesoporous Silica from Beach Sand by Sol-Gel Method as a Ni Supported Catalyst for Hydrocracking of Waste Cooking Oil

Siti Salamah[1], Wega Trisunaryanti[2*], Indriana Kartini[2], and Suryo Purwono[3]

[1]*Department of Chemical Engineering, Faculty of Industrial Technology, Universitas Ahmad Dahlan, Jl. Kapas No. 9, Semaki, Umbulharjo, Yogyakarta 55166, Indonesia*

[2]*Department of Chemistry, Faculty of Mathematics and Natural Sciences, Universitas Gadjah Mada, Sekip Utara, Yogyakarta 55281, Indonesia*

[3]*Department of Chemical Engineering, Faculty of Engineering, Universitas Gadjah Mada, Jl. Grafika No. 2, Yogyakarta 55281, Indonesia*

** **Corresponding author:***

tel: +62-811256055
email: wegats@ugm.ac.id

Received: November 13, 2021
Accepted: March 15, 2022

DOI: 10.22146/ijc.70415

Abstract: *Mesoporous silica (MS) supported by nickel was synthesized from Parangtritis beach sand and assessed for its activity and selectivity as catalysts in hydrocracking waste cooking oil into biofuel. The synthesis of MS was done by the sol-gel method. Ni/MS catalysts using Ni weight variations of 1, 5, and 10 wt.% were denoted as Ni/MS1, Ni/MS5, and Ni/MS10 and were compared to standard mesoporous silica (Ni/SBA-15). The catalysts were characterized using FTIR, XRD analysis, N_2 gas sorption analysis, SEM-EDX, and TEM. Catalyst Ni/MS1, Ni/MS5, Ni/MS10, and Ni/SBA-15 have specific surface areas of 130.5, 195.9, 203.9, and 381.2 m^2/g and the average pores of 12.30, 9.80, 11.12, and 8.70 nm, respectively. The hydrocracking was run four times to evaluate the catalyst reusability. The hydrocracking WCO has 95.8, 82.4, and 85.2%, respectively. While Liquid fractions produced were 38.8, 43.2, and 50.2 wt.%, each of which contains gasoline of 37.09, 39.76, and 44.27 wt.%, Ni/MS10 has the highest liquid products of 50.2 wt.% and was selective to gasoline fractions up to 44.27%. Therefore, the catalyst synthesized from Parangtritis beach sand is selective for gasoline-fraction hydrocarbon and has hydrocracking activity up to 4 runnings.*

Keywords: *beach sand; catalyst; hydrocracking; mesoporous silica; gasoline selective*

■ INTRODUCTION

The waste of cooking oil (WCO), one of the most frequently used cooking oils with over 3.5 MT/annum consumption (2.5% of world vegetable cooking oil production), can be considered a promising alternative for renewable energy sources [1]. The population growth per year led to increased cooking oil usage and, in turn, resulted in the accumulation of its waste in the environment [2]. Waste cooking oil (WCO) contains fatty acid methyl ester (FAME), which can be used as a biofuel. WCO can be environmentally friendlier than those made from food crops, such as palm oil. A suitable performing catalyst is required to convert a sufficiently high methyl ester content in WCO. The hydrocarbon produced from this process has similar compounds to those found in petroleum fuel, in which there is a higher energy density, lower viscosity, and higher stability [3].

Conversion of waste cooking oil into hydrocarbon requires an acidic catalyst with optimal activity, stability at high temperatures, and high selectivity for the desired product. Among many catalysts available, mesoporous silica has drawn much attention in recent years because of its high porosity properties and better performance [4]. However, the availability of MS and other synthetic silica materials is limited and may be expensive. The alternative is to use naturally occurring silica materials, such as beach sand. Beach sand is an example of carbonate sand with a silicon dioxide content of 72–84% [5], though the silica composition varies depending on

the geographical location. Parangtritis beach sand, located in Yogyakarta, Indonesia, abounds with silica [6]. For this reason, this research used silica extracted from Parangtritis beach sand as a material to synthesize mesoporous silica catalysts. However, no research has yet to confirm whether catalyst produced from beach sands has high activity and selectivity to hydrocarbon gasoline fraction.

Metal precursors are required to increase the number of active sites in a catalyst, thus increasing the activity and selectivity of the catalyst. This study impregnated nickel as metal precursors to support mesoporous silica catalysts. By impregnating nickel, it is expected to increase the number of active sites and the catalyst's ability, thereby increasing the catalytic performance. Nickel is also abundant, low cost, and environmentally benign.

This paper studied the synthesis of mesoporous silica from Parangtritis beach sand as a Ni-supported catalyst. The synthesis was done using a dodecyl-amine (DDA) template by sol-gel method, chosen for its relatively fast processing time, in addition to its low-temperature requirement, among other syntheses in the research study by Salamah et al. and Thahir et al. [6-7]. The nickel was then impregnated using the wet impregnation method with variations of nickel content weight of 1, 5, and 10 wt.%. The catalysts were assessed for the activity and selectivity in the hydrocracking process of waste cooking oil into gasoline fraction. The results were compared to the catalyst from standard synthetic mesoporous silica (SBA-15).

■ EXPERIMENTAL SECTION

Materials

The materials used in this study were silica extracted from Parangtritis beach sand, dodecyl amine supplied by Fisher Scientific, distilled water, HCl produced by Mallinckrodt, NaOH produced by VWR Chemicals, $AgNO_3$, C_5H_5N, Nickel nitrate, and silica standard produced by Sigma Aldrich, and SBA-15 produced by Green Stone Swiss Co. Ltd. Waste cooking oil was obtained collectively from the food shop.

Instrumentation

The functional group in silica, as well as the presence and disappearance of the DDA template from silica, was observed and analyzed using Fourier-Transform Infra-Red Spectrometer (FTIR) in combination with the KBr disc technique [8]. Surface Area & Pore Size Analyzer is from Quantachrome NOVA touch. The mesoporous silica crystallinity was analyzed using X-ray diffraction analysis, XRD-6000 Shimadzu. Morphology of mesoporous silica was characterized by Scanning Electron Microscope (SEM-EDX) mapping and Transmission Electron Microscope (TEM) JEOL JEM-1400 to analyze its pore structure [8]. The acidity of sand, silica, and mesoporous silica were analyzed using gravimetric base adsorption and hydrocracking WCO with a semi-fixed batch hydrocracking reactor.

Procedure

Extraction of silica from Parangtritis beach sand

The silica used was extracted from Parangtritis beach sand using the reflux method. The synthesis steps washed the sand to remove excess Cl and impurities. The washed sands were then sieved with 100 mesh, refluxed with 6 M HCl at 90 °C for 4 h, filtered, and washed with distilled water until the pH was 7. The neutralized sand was then dried at 120 °C for 2 h. Silica was extracted from the sand sample by refluxing each sample with 6 M NaOH at a constant temperature of 80 °C for 4 h, then filtered and washed. Concentrated HCl was added dropwise into the filtrate until the pH reached 12 and the solution turned white. The solution was then stored for 24 h until the gel was formed. Afterward, the gel was separated and washed until the filtrate had no Cl. The synthesized silica dried in an oven at 120 °C for 4 h [6].

Synthesis of mesoporous silica (MS)

Mesoporous silica was synthesized using the sol-gel method with DDA surfactant as a template [6]. First, powder SiO_2 was dissolved in a solution of 1.5 M NaOH and stirred at a temperature of 40 °C for 30 min to obtain soluble sodium silicate. Next, sodium silicate was added dropwise to 0.05 M DDA solution under rotation speed

of 120 rpm at room temperature and stirred for 40 min. The solution was left under a static condition at room temperature for 18 h [9]. The product was then filtered and washed with distilled water until the filtration reached a pH value of 6. Finally, it was dried at 50 °C for 4 h. The dried product was then calcined at 600 °C for 5 h with a heating rate of 5 °C /min to remove the surfactant template.

Synthesis of Ni/MS catalyst

The synthesized Nickel mesoporous silica (MS) catalyst was divided into three samples: Ni/MS1, Ni/MS5, and Ni/MS10, Ni/SBA-15 for the standard. The first sample, MS1, used Ni impregnation of 1 wt.%. Ni/MS5 and Ni/MS10 used nickel impregnation of 5 and 10 wt.%, respectively. The catalyst Ni/MS from mesoporous silica (MS) was prepared by impregnating nickel nitrate into MS for 24 h at 30 °C. The material was then dried in the oven for 24 h at 100 °C. Next, the catalyst was calcined at a temperature of 500 °C for 5 h under the flow of nitrogen gas (20 mL min^{-1}) and reduced for 4 h at 450 °C under the flow of H_2 (20 mL min^{-1}) for 3 h and then characterized by FTIR.

Sample characterization

The functional group in catalyst Ni/MS and the presence and disappearance functional group from MS were observed and analyzed using Fourier-Transform Infrared Spectrometer (FTIR) combined with the KBr disc technique, the sample used for analysis was 2–5 mg.

The acidity of catalyst Ni/MS was analyzed using gravimetric with pyridine as an adsorbate. An empty crucible was first dried in the oven at 100 °C for 1 h and weight as W1. As much as 0.1 g of the catalyst sample was put into the crucible, reheated at 100 °C for 1 h, and weighed as W1. As much as 0.1 g of the catalysts sample was put into the 100 °C for 1 h. The mass measured after this process was labeled as W2. The catalyst's crucible was then put into a closed desiccator and flowed with pyridine for 24 h. The mass of the sample obtained was considered W3. Total acidity is calculated using the following formula [10].

$$\text{Total Acidity} = \frac{W3 - W2}{(W2 - W1)\text{Mr}C_5H_5N} \times 1000$$

The catalyst was characterized using SEM, TEM, Surface Area, and Pore Size Analyzer.

The catalytic performance in hydrocracking waste cooking oil

Hydrocracking of waste cooking oil was done by putting 0.1 g of Ni/MS and 10 g of waste cooking oil into the oil container. The waste cooking oil sample and catalyst were put into a semi-fixed batch hydrocracking reactor [11]. The reactor with OD 25 cm, ID = 5 cm, length = 36 cm, holder feed at 10 cm long, OD 5 cm.

The catalytic activity of mesoporous silica was evaluated in hydrocracking waste cooking oil by a reactor. The reactor was set at a temperature of 450 °C, 1 atm, per 2 h, with a hydrogen gas flow at 20 mL/min. The liquid produced by hydrocracking waste cooking oil was further analyzed by Gas Chromatography-Mass Spectrometer (GC-MS, Shimadzu QP2010S) to determine the components of compounds in liquid products.

The reactant yield was determined gravimetrically by using calculation as written in the equation below [12]:

$$\text{Liquid fraction (LF) (wt.\%)} = \frac{Wp}{WF} \times 100\% \quad (1)$$

$$\text{Residue (wt.\%)} = \frac{WR}{WF} \times 100\% \quad (2)$$

$$\text{Coke (wt.\%)} = \frac{WC2 - WC1}{WF} \times 100\% \quad (3)$$

$$\text{Gas} = 100 - (\text{LF} + \text{coke} + \text{residue}) \quad (4)$$

$$\text{Total result (\%)} = (100 - \text{residue}) \quad (5)$$

$$\text{Selectivity (wt.\%)} = \frac{Ac}{AT} \times 100\% \quad (6)$$

where Wp is the weight of the product, WF is the weight feed, WR is the unconverted weight product (g), WC1 is the weight of catalyst before hydrocracking (g), WC2 is the weight of catalyst after hydrocracking (g), Ac is GC-MS area of the gasoline or diesel fraction or free fatty, aldehydes/ketones, alcohols and other oxygenates, and AT is the total GC-MS area.

■ RESULTS AND DISCUSSION

Characterization of Ni/Mesoporous Silica Catalyst

Functional Groups contracting all catalyst materials in this study were analyzed using FTIR, as shown in Fig. 1.

The broadband at a wavenumber of 460 cm^{-1} showed bending vibration, indicating the presence of Si–O–Si [13]. An influentially strong intensity band at 1090 cm^{-1} represented Si–O–SI stretching; this is due to the interaction of the O–H group originating from the water found on the Ni/MS surface through hydrogen bonds. It was generally known that the 450–1300 cm^{-1} range was the unique silica band [6]. The broadband at a wavenumber of 1632 cm^{-1} showed bending Si-OH as there were new bands at 1635 cm^{-1} and a strong band at 3437 cm^{-1}. This phenomenon follows a previous study by Qiu et al. and Komaruzzaman et al. [14-15]. The broadband at a wavenumber of spectra MS and Ni/SBA-15represented water O–H bending and O–H stretching, as well as silanol (Si-OH) and Siloxane functional (Si–O–Si), respectively [16]. The impregnation process of Ni does not destroy or affect the functional group of MS.

The materials used are mesoporous silica (either MS or SBA-15) which contains Si. Therefore the FTIR results show the presence of a Si bond toward OH (Si-OH) or Si–O–Si. A comparison of FTIR result analysis of MS with the Ni-supported catalyst does not show any significant difference. Similarly, the impregnation of Ni does not change the structure of MS. In addition, the FTIR result does not show any Ni peak because metal elements will only appear in the fingerprint area [16-17].

Acidity analysis

Ni/MS catalyst surface acidity was determined using pyridine as a base probe molecule in gravimetric analysis. The results were 0.71 mmol/g for sand, 0.9 mmol/g for silica,1.02 mmol/g for MS, 1.34 mmol/g for Ni/MS1 and 1.55 mmol/g for Ni/MS5, Ni/MS10 1.74 and Ni/SBA-15 2.09 mmol/g. The higher acidity of Ni/SBA-15 and Ni/MS10 showed potential as a catalyst that requires acid sites, such as hydrocracking. The greater the nickel impregnation, the higher the acidity was. This property was due to the uneven distribution of the pores on the layer surface of the material [14,18-19].

The data show that the Ni/MS catalyst had a higher total acidity value than the MS. The increase in total acidity was caused by metals deposited on the carrier, resulting in more acidic sites. The number of acidic sites affected pyridines adsorbed on the catalyst surface. In addition, the increased metal contents led to more acidic sites, which in turn increased the probability of pyridine adsorption on the catalyst surface. This phenomenon showed that Ni/MS catalysts could be used as hydrocracking catalysts.

Catalyst crystallinity analysis

The catalyst crystallinity was examined using XRD (Fig. 1). Sand and silica have crystalline, Excluding Ni/MS1, Ni/MS5, and Ni/SBA-15. It was found that MS has an amorphous silica mesoporous phase [16]. In contrast, the catalyst with impregnated Ni 10 wt.% showed crystals. This crystalline structure was because the increase in the metal content of Ni produced a crystal diffractogram pattern with crystal peaks appearing at 2θ = 44, 52, and 76° (111), (200) and (220) (JCPDS card

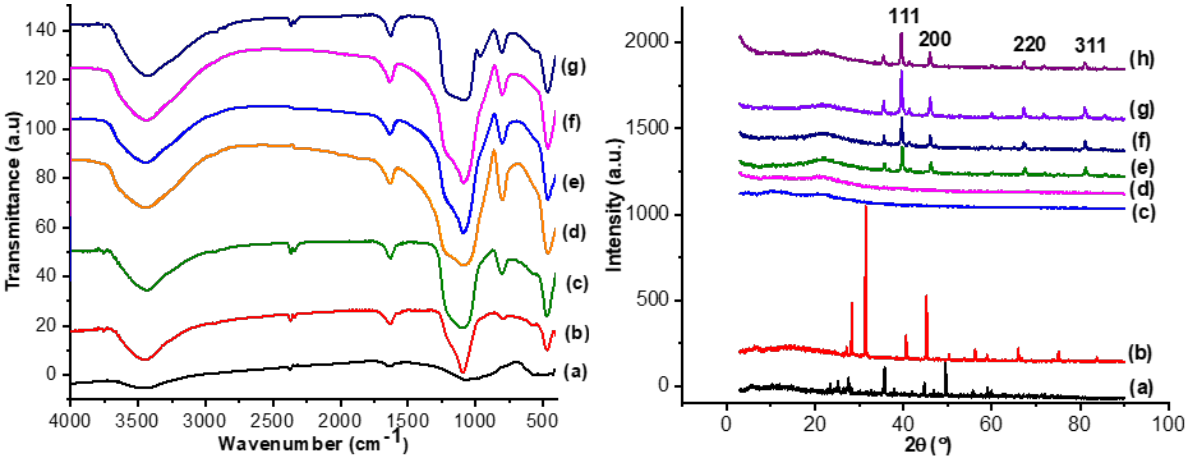

Fig 1. Infra-red spectra (left) and diffraction pattern (right) of (a) Sand, (b) Silica, (c) MS, (d) Ni/MS1, (e) Ni/MS5, (f) Ni/MS10, and (g) Ni/SBA-15 catalyst

no. 00-004-0850). These results indicate that these peaks are characteristic of Ni where the presence of sufficient nickel oxide forms face-centered cubic Ni crystals, which aligns with a research study by Sudhasree et al. [16]. When the Ni impregnation on MS is conducted, this stage can be explained as follows:

$Ni(NO_3)_2.\ 6\ H_2O_{(s)} + H_2O_{(l)} \rightarrow Ni^{(2+)}\ (aq) + 2\ NO_3^- + 7\ H_2O_{(l)}$

When immersed in the carrier system, Ni precursors in the form of cations (Ni^{2+}) with high mobility were adsorbed into MS solids due to the chemical potential difference between the solution and MS solids. Subsequently, the cations interacted with MS (carrier) and were distributed in the material. There was a coordinated covalent bond between the Ni^{2+} ion and the oxygen atom on the MS surface (carrier 0 to form NiO) after the calcination treatment. The reduction treatment using H_2 gas resulted in a great NiO bonded to the MS surface being reduced to aggregate Ni particles [19-20],

$NiO(S) + H_2\ (g) \dashrightarrow Ni(s) + H_2O\ (g)$

Morphology of Ni/MS1, Ni/MS5, Ni/MS10 catalyst

SEM was used to further confirm the morphological structure of the synthesized material at a magnification of 5000 times with an energy of 15 kV. EDX was used to determine the amount of impregnated Ni concentration. The morphology of sand, silica, MS, Ni/MS1, Ni/MS5, Ni/MS10, and Ni/SBA-15 are shown in Fig. 2, Table 1, and Fig. 3.

The SEM image catalyst in Fig. 2. shows the morphology of (a) sand, (b) silica sand, (c) mesoporous silica, (d) Ni/ MS1, (e) Ni/MS5, (f) Ni/MS10, and (g) Ni/SBA-15, which are uniformly bundled macroscopic structures. The figure reveals that the surface of the catalyst material is rough and consists of a relatively uniform arrangement of particle aggregates. The shape is almost spherical (semispherical), in which the agglomeration of the particle aggregates containing Ni is higher than that of MS. Typical particle agglomerates in the form of granules formed on the Ni/MS5 catalyst are

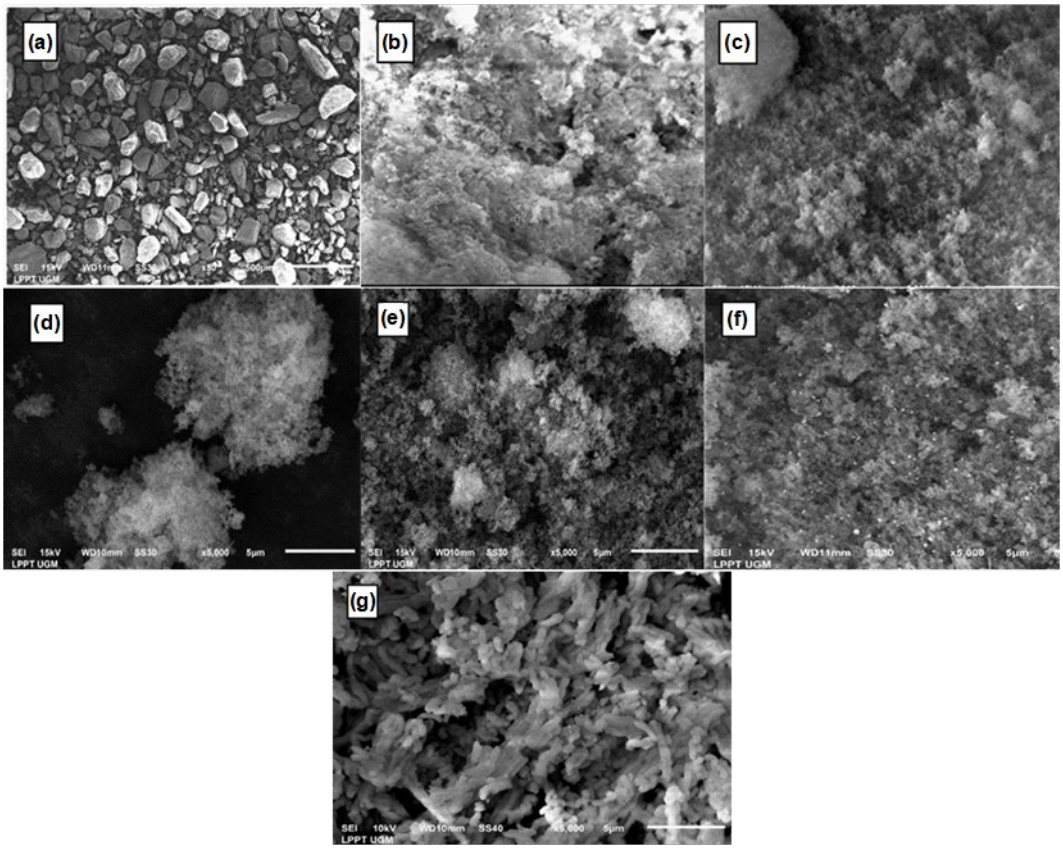

Fig 2. Morphology of catalyst (a) Sand, (b) Silica, (c) MS, (d) Ni/MS1, (e) Ni/MS5, (f) Ni/MS10, (g) Ni/SBA-15

larger and more non-uniform than those on MS. Small particles tend to form strong agglomerates, which require very high specific energy inputs to overcome the adhesion forces between particles.

The morphology type of MS is an aggregate shaped like a coral, while the morphological type of Ni/SBA-15 is an aggregate that is shaped like a rod [19]. On the surface of the MS catalyst, all MS pores are visible, which is characteristic of amorphous carrier material. In the Ni/MS1 and Ni/MS5 pictures, agglomeration of the impregnated metal appears to occur.

In Ni/MS10, the impregnated Ni metal enters the pores and spreads evenly on the catalyst surface. This phenomenon is related to the results of the XRD analysis that the metal-bearing Ni is 10%, as also evidenced in the previous research by Komaruzzaman et al. [15]. The characteristics of Ni have embedded in a porous material forms Ni, which is in the pores and on the surface of the pores, causing agglomeration [19]. The element on the surface of Ni/MS1, Ni/MS5, Ni/MS10, and Ni/SBA 15 were analyzed by EDX mapping, as shown in Table 1 and Fig. 3.

Not all the Ni content on the surface of the impregnated mesoporous silica can be deposited. At 1% impregnation Ni, 0.87% impregnated Ni, the higher the impregnated Ni, the lower the impregnated metal was. This effect was probably due to the agglomeration of Ni metal and the amount of Ni on their surface, which were dramatically different. This indicated that most Ni in Ni/MS5 entered and filled the pores or the internal surface of the materials, and hence, they did not appear on the surfaces [20].

The EDX mapping is a beneficial method for examining the distribution of each type of atom on the catalyst's surface. As shown in Fig. 3. the EDX spectra confirm that the main elements of the analyzed material are Silica (Si), Oxygen (O), and Nickel (Ni). The EDX data shows that the Ni/MS catalyst material contains several elements. The ratio of the mass percent of the elements Si, O, and Ni are presented in Table 1. The catalyst material prepared with the highest concentration contains 5.96% Ni. The EDX analysis data

Table 1. Element contents of catalyst

Sample	Element composition (wt.%				
	Si	O	C	Na	Ni
Ni/MS1	27.31	48.72	22.3	0.73	0.87
Ni/MS5	27.21	67.56	0	1.21	0.64
Ni/MS10	33.19	54.47	0	1.41	5.96
Ni/SBA-15	33.50	50.91	13.89	0	0.46

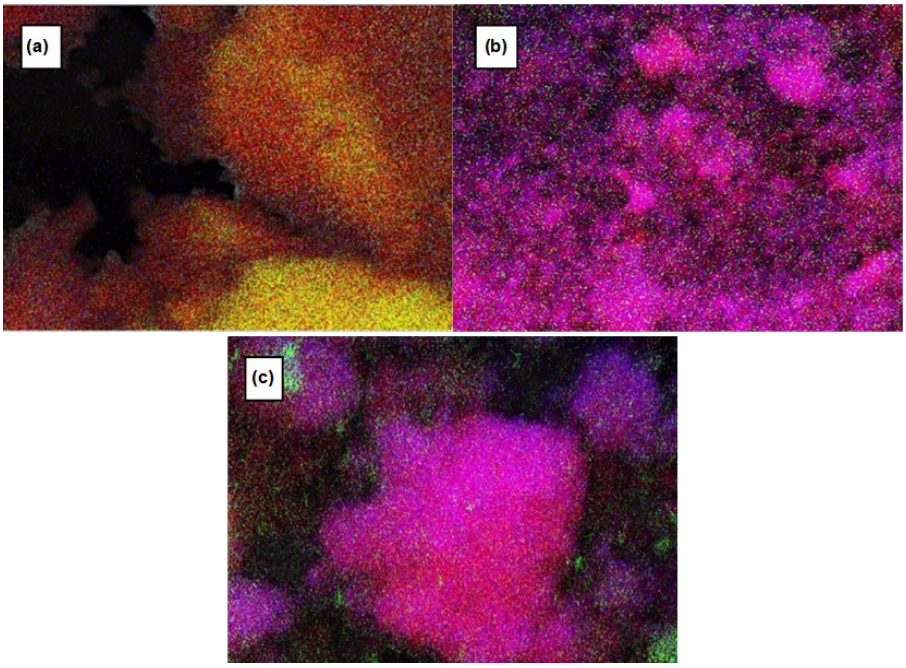

Fig 3. EDX-Mapping morphology of (a) Ni/MS1, (b) Ni/MS5, and (c) Ni/MS10 catalyst

listed in the picture (which is colorful) is a mapping of the distribution of Si, O, and Ni elements on the surface of the Ni/MS catalyst material. The mapping shows that the dispersion of silica and oxygen, and Ni on the catalyst's surface is relatively homogeneous, and agglomeration occurs.

In the Ni/MS1 catalyst, the red, green, and blue colored dots are identified as silica, oxygen, and nickel. The Ni is evenly distributed. In the Ni/MS5 and Ni/MS10 catalysts, the red, blue, and green colored dots are identified as silica, oxygen, and nickel. This shows that the Ni atoms are evenly distributed. However, there is an agglomeration of the Ni atoms in clusters. The agglomeration is not expected because it reduces the surface area of the catalyst, which is expected to interact with the feed during the catalyst activity test. This finding is in line with previous studies by Qiu et al. [14] and Wang et al. [19]. Ni atom precursors are difficult to direct into the mesoporous channels. Ni is detected both inside and outside the pores, causing poor dispersion due to redistribution and agglomeration. This finding is in line with previous studies by Pauly et al. [21].

Gas sorption analysis catalyst

The synthesized catalyst Ni/MS were analyzed using Gas Sorption Analyzer (GSA) to determine their porosity character. In this analysis, the isotherm graph and specific surface area were calculated using the BET equation. Pore volume, average pore diameter, and pore size distribution were calculated using BJH.

The characterization of GSA produced the classification of mesoporous materials based on their pore size according to the material classification [22-23]. The results of the characterization of GSA can be seen in Table 2.

The results show that Ni/MS catalysts and MS have a larger surface area than sand and silica. MS also shows 122.8 m^2/g, which indicates that it is a mesoporous material. Based on this data, it can be concluded that the synthesis of MS from the DDA template and Parangtritis beach sand was successfully carried out.

The Ni impregnation into MS increases the surface area of MS; the more significant the Ni is carried, the wider the surface area becomes. For example, for 10 wt.% Ni, there is an increase of 60% in the surface area. Ni/MS10 has a surface area of 203.9 m^2/g, while Ni/SBA-15 has 381.2 m^2/g. As the surface area increases, more reactants are adsorbed, and the possibility of a reaction occurring is more significant. The impregnation of Ni causes an increase in the physical properties of the catalyst into the MS pores as the entry of Ni into the carrier increases the active site. The acidity triggers the increase. The higher the Ni content is, the more the active sites are formed.

Similarly, the greater the total Ni content is, the wider the surface area becomes, as well as the greater pore volume. This phenomenon is probably due to the Ni being evenly distributed in the carrier system even though there is a slight buildup at certain pore channel positions. The adsorption-desorption isotherm of N_2 gas on the surface of the Ni/MS catalyst is shown in Fig. 4. The desorption isotherm shows a hysteresis loop starting at a P/P_0 relative pressure of about 0.5. This fact indicates that the relative pressure is brought to 0.5. Nitrogen gas is adsorbed on the monolayer. When the relative pressure starts to be in the range of 0.5 to 1, a multilayer arrangement of nitrogen gas occurs on the active Ni/MS surface. The adsorption isotherm is typical of a reversible type IV with hysteresis loop based on the

Table 2. The porosity property of the Ni/MS catalyst

Samples	Specific surface area (m^2/g)	Total pore volume (cm^3/g)	Average pore diameter (nm)
Sand	1.08	0.003	2.47
Silica (S)	9.4	0.006	19.12
MS	122.8	0.14	4.65
Ni/MS1	130.5	0.37	12.30
Ni/MS5	195.9	0.47	9.80
Ni/MS10	203.9	0.52	11.12
Ni/SBA-15	381.2	0.80	8.70

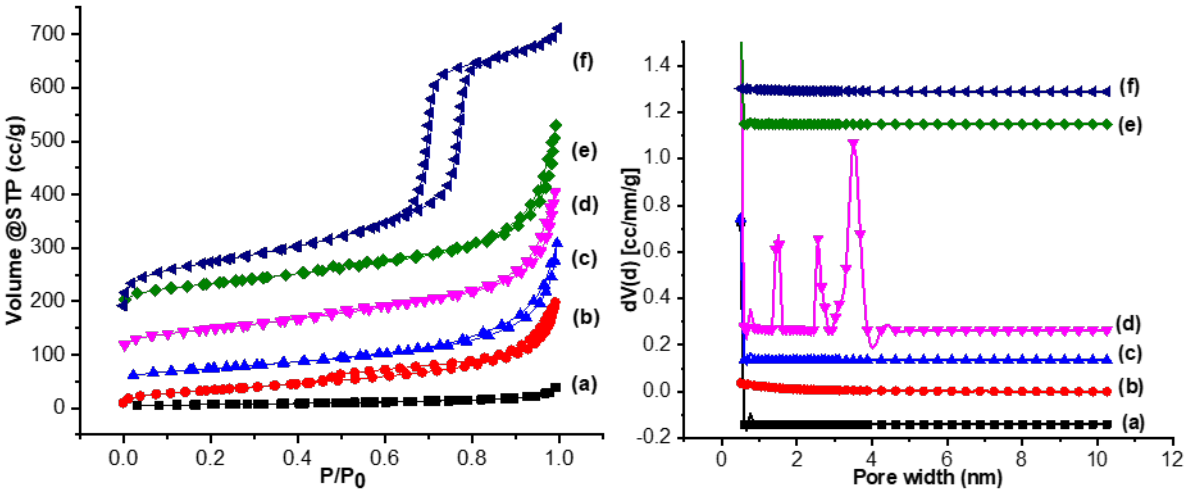

Fig 4. Adsorption-desorption isotherm graphs (left) and pore size distribution graphs (right) of the (a) Silica, (b) MS, (c) Ni/MS1, (d) Ni/MS5, (e) Ni/MS10, and (f) Ni/SBA-15 catalyst

IUPAC classification Schemer for Mesoporous materials [14,23] is shown in Fig. 4.

The hysteresis loop formed in the desorption adsorption isotherm has an HIV pattern. The HIV hysteresis loop indicates that the Ni/MS catalyst has a smaller pore mouth size than the pore body size, referred to as a bottle-shaped pore. The bottle-shaped pore causes the nitrogen gas desorption process to run faster. As a result, the amount of nitrogen gas adsorbed and adsorbed at the same pressure is much different. The increase in pore diameter is caused by the space between the layers of the crystal lattice planes, which increases the distance between the crystal lattice planes and causes an increase in the pore diameter. The expansion of the metallic Ni in MS causes the diameter range to increase and allows more gas molecules to enter, thus causing the formation of a more porous structure between layers and contributing to an increase in surface area and porosity. All the three catalysts have the same mesoporous, which is characterized by the presence of a hysteresis loop [22-23].

As shown in Fig. 4, the Ni/MS1, Ni/MS5, and Ni/MS10 catalysts have a reasonably wide pore size distribution, ranging from 1–10 nm. This pore size corresponds to the pore size range of the mesoporous material, which is 2–50 nm [23]. The pore size distribution is the relative abundance of each pore size based on the sample volume represented as dv/r, where this function has a value that is proportional to the combined volume of all pores whose effective radius is in a minimal range and centered on r. The Ni/MS pore size distribution profile synthesized with variations in Ni mass indicated the presence of a small number of pore fractions with a pore diameter of 4–12.3 nm. The catalyst Ni/MS1, Ni/MS10, and Ni/SBA-15 showed a homogeneous pore distribution of solids. As for the Ni/MS5 catalyst, the pore size distribution is tapered at a diameter of 1–4 nm and slopes at 4–9.8 nm. This catalyst is characterized by mesoporous solids with the most abundant heterogeneous pore distribution at 2–4 nm in diameter. The presence of micropores causes a decrease in pore diameter, which becomes smaller than the Ni/MS10 catalyst. This is probably due to the Ni/MS5 catalyst, where many impregnated Ni agglomeration occurs on the catalyst's surface. The pore distribution is more diminutive than Ni/MS1 and Ni/MS5, as supported by SEM EDX data. This data indicates that the Ni/MS5 obtained is micropore and mesopore-sized, referred to as hierarchical mesoporous [16]. These types follow the data in Fig 3.

Characterization using TEM

TEM image is required to ensure that the synthesized MS has pore gaps according to the results of the GSA analysis. The TEM image in Fig. 5 appears to have clear pores like wormholes. The use of nickel made

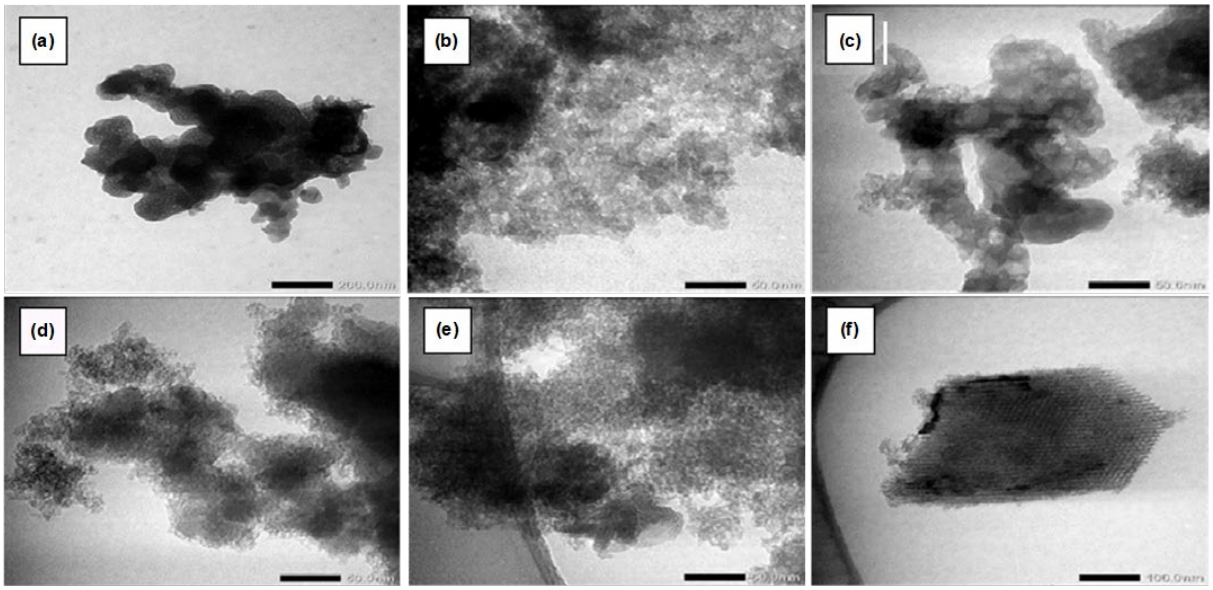

Fig 5. Morphology TEM of (a) silica, (b) MS, (c) Ni/MS1, (d) Ni/MS5, (e) Ni/MS10 and (f) Ni/SBA-15 catalyst

the pore structure of Ni/MS irregular. Pores with a wormhole-like structure were obtained [4,24]. TEM images are required to ensure that the synthesized Ni/MS has a pore gap according to the results of the GSA analysis.

The presence of Ni forms more pores with an irregular pore shape similar to a wormhole, as revealed in previous research studies [4,24]. As a result, the surface area becomes more prominent, and the pore radius increases. The number of pores formed due to the spread of Ni leads to the increasing pore volume in proportion to the added Ni. The study results using variations in the percentage of Ni showed a significant change in the catalyst's performance obtained. As shown in Fig. 3, a severe degree of agglomeration occurs with the addition of 10% Ni. In the results of Ni, which was impregnated with SBA-15, it was also seen that the metal agglomerated in several places.

Catalytic Performance in Hydrocracking of Waste Cooking Oil

This study tested the catalytic activity of MS, Ni/MS1, Ni/MS5, and Ni/MS10 catalysts. The bait used in this research was waste cooking oil. The hydrocracking process was carried out at a temperature of 450 °C and with the weight ratio of catalyst: feed 1:100 and H_2 gas flowed with a flow rate of 20 mL/min to find the catalyst with the best activity and selectivity. The catalytic activity can be seen in Table 3. The Ni/MS10 has a higher surface area than silica, Ni/MS1, and Ni/MS5. Ni/MS1, Ni/MS5, and Ni/MS10 shows a liquid fraction of 38.8, 43.2, and 50.2 wt.%.

The Ni/MS 10 catalyst produces the highest liquid product. This result is due to the entry of Ni into the pores of MS. Furthermore, Ni/MS has an active site that helps the hydrocracking process. Ni in the hydrocracking process is used as the active site due to its unpaired electrons in the d orbitals. The unpaired electron in the d orbital homolitically dissociates hydrogen gas required in the hydrocracking process and functions as an active hydrogenation site and a Brønsted-Lowry acid site [15]. The Ni/MS10 catalyst has a higher liquid product than the MS due to its higher acidity value. The higher acidity value of a catalyst results in a higher liquid product. This is because an increase in the total acidity of a catalyst causes an increase in the number of acid sites. Whereas the number of acid sites also attracts hybrid ions (H^+), which play a role in the initial stage of the hydrocracking process. This finding aligns with the previous research study by Qiu et al. [14], who state that a high total acidity increases the liquid product in the hydrocracking process.

Similarly, the presence of Ni reduces the gas product. The used waste cooking oil has been successfully

Table 3. Hydrocracking products of waste cooking oil

Hydrocracking catalyst	Result (wt.%)				Total result (wt.%)
	Liquid product	Gas product	Residue	Coke	
Thermal	15.2	57.3	27.5	0	72.5
MS	41.2	51.2	6.2	1.4	93.7
Ni/MS1	38.8	55.3	4.2	1.7	95.8
Ni/MS5	43.2	37.8	17.5	1.9	82.4
Ni/MS10	50.2	33.3	14.8	1.7	85.2
Ni/SBA15	46.7	40.3	11.3	1.7	88.7

converted into a liquid product [25]. Therefore, the Ni/MS1 catalyst decreases while the amount of gas formed increases. This is probably due to the metal Ni/MS1 catalyst not being well distributed. During the agglomeration, the waste cooking oil, as the feed, cannot be desorbed by the catalyst or is retained on the catalyst so that it causes gas formation. This finding aligns with the previous studies on catalytic performance [13,20].

The main components of used waste cooking oil are petroselinic acid and palmitic acid, where C18 and C16 of the two fatty acids are cracked into shorter hydrocarbon chains if the oxygen is removed, or vice versa, creating shorter fatty acid chains [8]. In the hydrocracking process, the waste cooking oil is converted into liquid, gas, and coke fractions, as shown in Table 3. Ni/MS10 catalyst shows superior performance in producing liquid fraction while retaining its ability to avoid over-cracking, as indicated by the relatively low gas fraction produced. This phenomenon can be caused by the excellent catalyst pore structure, where the mesopores on the catalyst surface allow the feed to enter the catalyst while releasing the product easily.

Liquid product produced in thermal cracking is less compared to catalytic hydrocracking. Thermal cracking produces more gas products compared to catalytic hydrocracking as a result of radical ion formation affected by relatively high temperatures. Radical ions formed in the initiation stage of thermal cracking break the carbon bond and form a new radical compound with fewer carbon atoms; hence, more gas product is produced than catalytic hydrocracking. According to Kusumastuti et al. [24], catalyst Ni/MS10 produces the most liquid product of 50.2 wt.%. This occurrence is due to the penetration of the optimum metal composition of Ni to the MS pores. Ni also has active sites, which helps the hydrocracking process. In the hydrocracking process, Ni is used as the active site because of unpaired electrons in the d-orbital. Unpaired electrons in the d-orbital will dissociate hydrogen gas homolytically, which is required in the hydrocracking process, and function as active hydrogenation sites and as acid sites of Brønsted-Lowry.

The study shows that the surface area was higher, and the location of the acid site could be responsible for this phenomenon, where the acid site of Ni/MS may reside deep beneath the catalyst. While the feed and product could come in and out easily, the chance of the feed finding the active site before they exit the catalyst becomes slimmer. This hypothesis seems to be responsible for the relatively high amount of oxygenated product [24,26]. The more Ni is impregnated, the more the active sites will be. However, the increase of Ni impregnated can cover the catalyst pore, which causes Lewis's acid site to be clogged, which causes agglomeration. This agglomeration process makes it difficult for the feed in the hydrocracking process to find the active site on the catalyst, compared to the condition of evenly distributed metal and minimal agglomeration. The evenly distributed metal causes the feed to be on the active surface of the catalyst, which may cause the breaking of the C=O bond to produce alcohol as an intermediate. Further hydrogenation of the alcohol produces long-chain hydrocarbons via the hydrodeoxygenation mechanism, as revealed in previous research studies [27]. The Ni/MS catalyst is the most optimal as it has 50.2 wt.% in the liquid fraction, and the thermal reaction has a liquid product of 15.2 wt.%. The results of the analysis of liquid products from hydrocracking show that thermal cracking produces

Table 4. Selectivity of the Ni/MS1, Ni/MS5, and Ni/MS10 catalyst

Hydrocracking catalyst	Liquid fraction (wt.%					
	Gasoline (C_5-C_{12}	Diesel (C_{13}-C_{17}	Free fatty acids	Aldehydes/Ketones	Alcohols	Other oxygenates
Thermal	1.08	7.64	0.00	3.36	3.13	0.00
MS	22.9	1.00	5.34	5.60	5.69	0.66
Ni/MS1	37.09	0.00	0.17	0.41	0.24	0.78
Ni/MS5	39.76	0.24	0.63	0.38	0.24	1.96
Ni/MS10	44.27	0.51	2.57	1.37	1.46	0.00
Ni/SBA15	31.10	0.77	4.94	5.59	1.06	3.25

Gasoline is hydrocarbons containing C_5 to C_{12} atoms,
Diesel is hydrocarbons containing C_{13} to C_{17} atoms,
Oxygenates contain ether, silane, epoxy

1.08% gasoline and 7.64% diesel. Hydrocracking with a catalyst, there is an increase in liquid products containing gasoline from 31.1 to 44.27%. This increase shows that the impregnation of Ni influences the cracking process and that Ni carriers in MS can undergo deoxygenation, decarboxylation, and decarbonylation reactions [26,28-29].

In this study, the liquid product was analyzed using GC-MS (see Table 4). The Gas Chromatography (GC) serves as a separator, while the Mass Spectrometer (MS) was used to detect liquid faction. The analysis of the chromatogram data produced by the gas chromatography shows the number of components that were separated from the liquid fraction and were detected using a mass spectrometer (MS). The liquid product was obtained from the hydrocracking process of waste cooking oil. This finding is in line with previous studies by Nugraha et al. [25].

The catalyst obtained in this synthesis is selective for the gasoline fraction, the most selective being the Ni/MS10 catalyst. It is probably due to the large surface area and high acidity. The increase in total acidity occurs because the Ni deposited on the carrier provides acidic sites. The acidity and contribution of different catalysts create catalysts with different activities and selectivity. A suitable condenser is required for the hydrogenation of oxygen-containing components. The pore size in the mesoporous catalyst region helps the reactants and intermediates overcome the limited diffusion of adsorption at the Ni sites [9,13].

Several reactions coincide in the cracking process with a catalyst. The cracking occurs by breaking the C–C bond in the compound. According to Yıldız et al. [3] and Chen et al. [29], the cracking reaction of used waste cooking oil goes through 3 stages, namely decarboxylation, decarbonylation, and hydrodeoxygenation, as shown from the reaction pathway in Fig. 6 [29].

Furthermore, through decarboxylation, CO_2 by-products are formed. The decarboxylation and hydrodeoxygenation reactions often occur through a catalyst following the fatty acid deoxygenation process. The decarboxylation and hydrodeoxygenation reactions coincide to form alkane and alkene products. The number of particular products for the chain gasoline fraction with carbon atoms is from 5 to 12 (C_5–C_{12}). These products show that the hydrodeoxygenation and decarboxylation reactions may occur with hydrogen gas flow at a rate of 20 mL/min [19,26]. The results of the hydrocracking process are in Table 4 and Fig. 7. Hydrocracking with a catalyst, there is an increase in liquid products containing gasoline from 31.1 to 44.27%.

In thermal cracking, relatively few gasoline compounds are formed compared to diesel, and aldehyde and alcohol were formed. In the hydrocracking of WCO with a Ni/MS1 catalyst, several alkane compounds are isomers of hydrocarbon compounds. At peak numbers 15, 19, 20, and 25, a compound with the molecular formula $C_{11}H_{22}$ is 2-Undecene (Z), 1-Undecane, 3-Undecane (Z), and 3-Undecane. At peak 27, 34, and 36 are compounds with the molecular formula $C_{12}H_{24}$, namely 5-5-Dodecane, E1-Dodecane, and Cyclohexane. According to Chen et al. [29], the

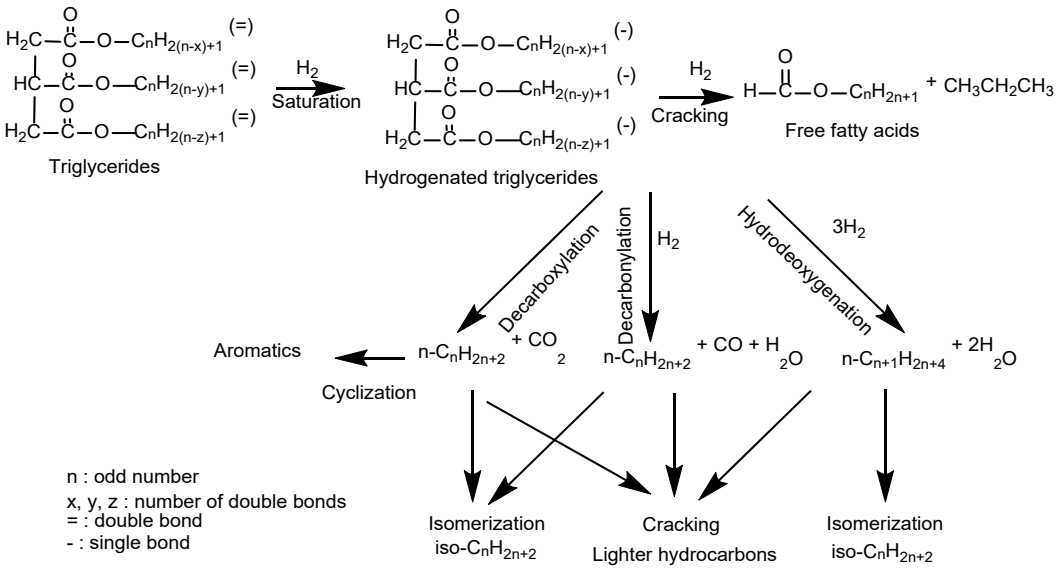

Fig 6. The possible hydrocracking pathway

Table 5. Distribution of catalyst reusability in hydrocracking WCO

Catalyst	Result (wt.%				Total result
	Liquid product	Gas product	Residue	Coke	(wt.%
Ni/MS1[1]	38.8	55.3	4.2	1.7	95.8
Ni/MS1[2]	38.3	27.6	32.1	2	67.9
Ni/MS1[3]	39.9	32.1	26.1	2	73.9
Ni/MS1[4]	49	34.8	12.4	3.8	87.6
Ni/MS5[1]	43.2	37.8	17.5	1.9	82.4
Ni/MS5[2]	37.7	33.8	27.2	1.3	72.8
Ni/MS5[3]	46	28.9	22.5	2.6	77.5
Ni/MS5[4]	41.8	42	15.9	0.3	84.1
Ni/MS10[1]	50.2	33.3	14.8	1.7	85.2
Ni/MS10[2]	37.8	29.8	31.5	0.9	68.5
Ni/MS10[3]	25.5	52.7	20.9	0.9	79.1
Ni/MS10[4]	40.7	19	34.1	1.3	81
Ni/SBA15[1]	46.7	40.3	11.3	1.7	88.7
Ni/SBA15[2]	48.9	27.9	21.1	2.1	78.9
Ni/SBA15[3]	46.6	30	22.3	1.1	77.7
Ni/SBA15[4]	43.1	52.6	2	2.3	98

[1]The first hydrocracking; [2]The second hydrocracking; [3]The third hydrocracking; [4]The fourth hydrocracking

formation of this isomer is due to the decarboxylation and hydrodeoxygenation processes.

The reusability of Ni/MS1, Ni/MS5, and Ni/MS10 catalyst for hydrocracking of WCO

The stability test of the Ni/MS catalyst was conducted 4 times for hydrocracking using WCO at a temperature of 450 °C and a weight ratio of 1:100 catalyst: feed. Throughout 4 testing runs, the Ni/MS1, Ni/MS5, and Ni/MS10 catalysts produced optimum activity and selectivity with high conversion rates. The results of the reusability of the catalyst can be seen in Table 5. The Ni/SM5 catalyst activity increased with the use of the catalyst throughout the four runs. The GC-MS

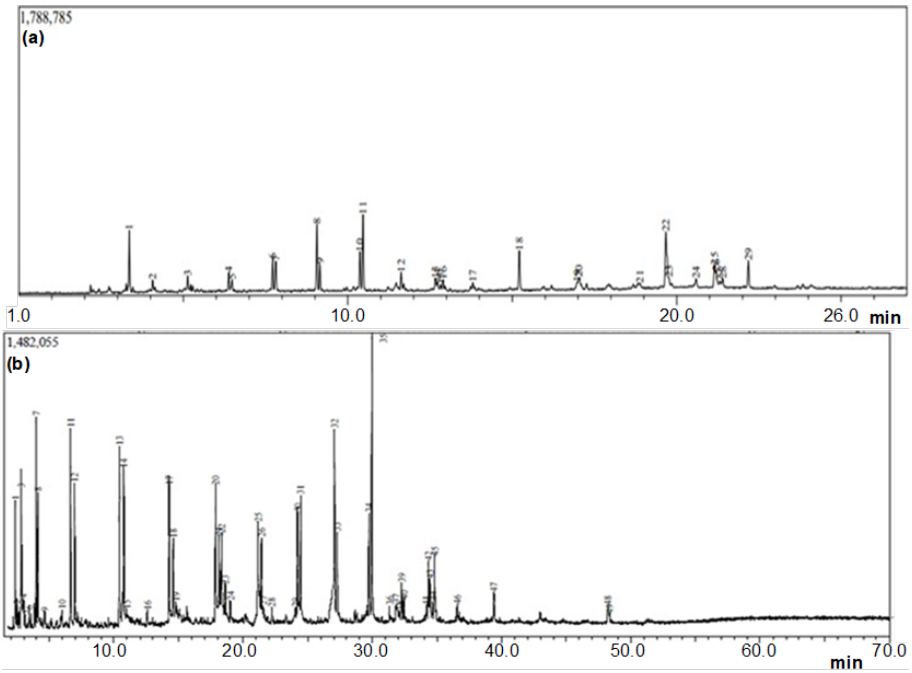

Fig 7. The Gas chromatograms of (a) thermal cracking WCO and (b) hydrocracking WCO with Ni/MS1

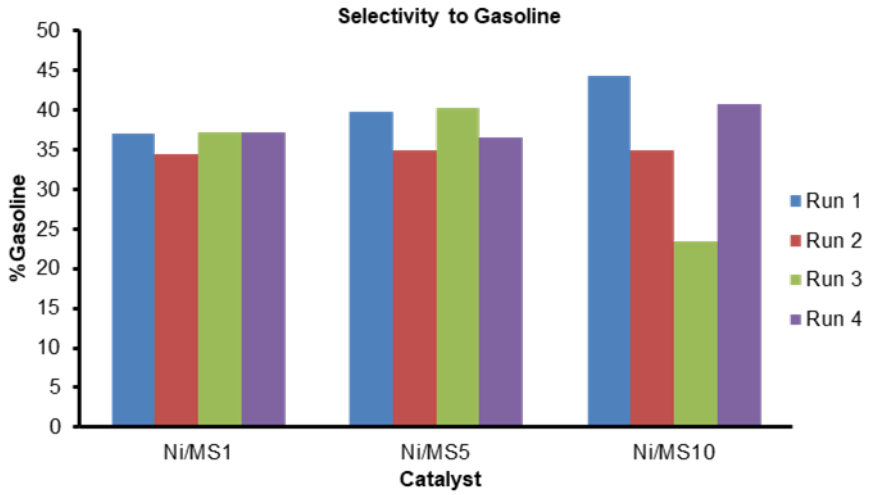

Fig 8. The reusability of catalyst from hydrocracking of WCO

analysis of reusability results can be seen in Fig. 8.

The stability test results of GC-MS analysis on selectivity in the gasoline fraction show that the Ni/MS5 and Ni/MS10 catalyst is relatively stable throughout the four runs. This stabilization effect is probably due to the overall character of the catalyst, namely Ni properties, acidity, surface area, pore volume, pore diameter, and reaction mechanism. The Ni/MS10 catalyst has the highest acidity and surface area. Coke formation was also seen to decrease, indicating stability against coke poisoning. Increasing the amount of coke on the catalyst's surface can cover the catalyst's active site where the deoxygenation mechanism occurs. The deactivation of the catalyst that occurs is caused by the formation of coke deposited on the active site of the catalyst. The residue increased with the reuse of the Ni/MS catalyst.

The results of the repetition of the Ni/MS10 catalyst were seen decreasing in the 1st, 2nd, and 3rd run and

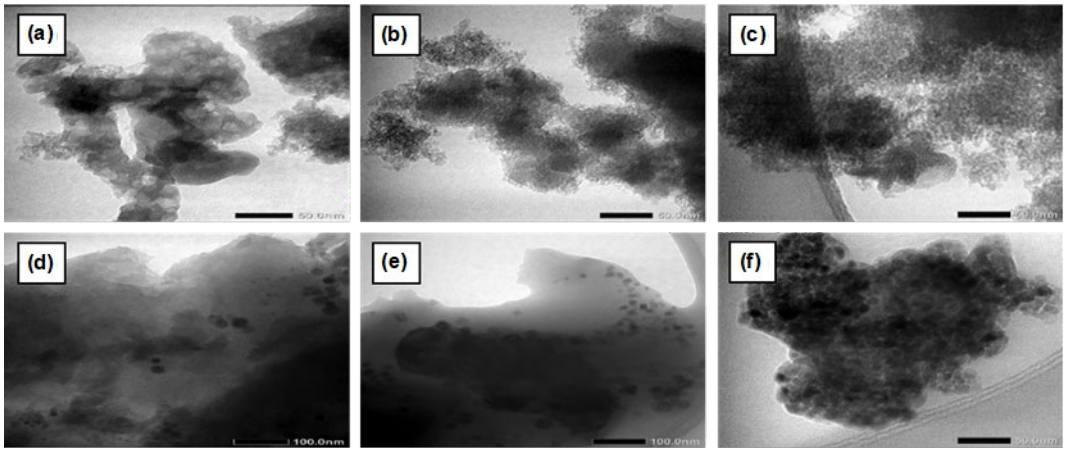

Fig 9. Morphology TEM of catalyst before and after hydrocracking

they were increasing in the 4th run. According to Trisunaryanti et al. [27] and Rodiansono and Trisunaryanti [28], after repeated use of the catalyst, the active sites decrease either due to coke or temperature. The reduction of the active site causes the hydrocracking reaction to being more dominantly affected by temperature than by the catalyst. At the same time, this increase is due to the polymerization reaction of lighter components into components with a more significant number of carbon atoms. Although still going through the mechanism of free radical formation, these radicals combine to form more significant hydrocarbon compounds.

The morphological structure of the Ni/MS catalyst before and after the stability test in this study was characterized using a Transmission Electron Microscope (TEM) observed at 100 nm magnification. The Ni/MS catalyst before and after hydrocracking is shown in Fig. 9. As can be seen, Fig. 9(a–c) are the catalysts before hydrocracking when the agglomeration has not occurred. Fig. 9(d–f) shows the condition after the fourth use when black spots and clumping appear. Clumping that occurs indicates the presence of a sintering process. The sintering process can occur due to too high a temperature, which causes the aggregation of Ni [24-25]. The black stain that is visible comes from the nickel getting darker. It indicates that coke formation affects the deactivation of the catalyst [12]. This result also follows the coke level in Table 3, which shows the increasing amount of coke, and in Fig. 9(e) and 9(f), which indicate quite dark black spots. Coke formation was also seen to increase, indicating stability against coke poisoning. Increasing the amount of coke on the catalyst surface can cover the active catalyst site where the deoxygenation mechanism occurs. The deactivation of the catalyst that occurs is caused by the formation of coke deposited on the active site of the catalyst. The residue increased with the reuse of the Ni/MS catalyst.

Coke is a by-product formed during the hydrocracking process. Coke can reduce the activity of the catalyst because coke can cover the active site of the catalyst, causing the breakdown of long-chain hydrocarbons to be lower. This produced coke causes a decrease in the activity of the catalyst, as can be seen in the picture on the stability test. Trisunaryanti et al. [12] reused the catalyst as several acid sites became shields from the coke deposit.

■ CONCLUSION

The Ni/mesoporous silica catalyst was successfully synthesized from Parangtritis Beach sand using dodecyl Amina as a template. The catalysts were synthesized by impregnating MS with Ni metal of 1, 5, and 10 wt.% weight variations and were denoted as Ni/MS1, Ni/MS5, and Ni/MS10. These catalysts had specific surface areas of 130.5, 195.9, and 203.9 m^2/g, while standard Ni/SBA-15 had 381.2 m^2/g. The average pores were 12.30, 9.8, and 11.12 nm, while Ni/SBA-15 had 8.7 nm. The hydrocracking WCO has 95.8, 82.4, and 85.2 wt.%, and Ni/SBA-15 88.7 wt.%. The activity catalyst produced

liquid fractions recorded at 38.8, 43.3, 50.2, and 46.7 wt.%. They respectively contain gasoline (C_5–C_{12}) of 37.09, 39.76, and 44.27% and Ni/SBA-15 has 31.10%. Therefore, it could be deduced that Ni/MS10 has exceptional performance with reusability until 4 times running and still produce gasoline of 40.73 wt.%. Therefore, the catalyst synthesized from Parangtritis beach sand is selective for gasoline-fraction hydrocarbon and has hydrocracking activity up to 4 runnings.

■ ACKNOWLEDGMENTS

The authors would like to express the deepest gratitude to the General Director of Higher Education, Ministry of Education and Culture Indonesia, for the financial support under the scheme of Universitas Gadjah Mada Doctoral Dissertation Research (PDD) grant with a contract number 208/UN.1/DITLIT/DITLIT/PT/2021).

■ AUTHOR CONTRIBUTIONS

The first author conducted the experiment, data collection, and analysis and drafted the manuscript. The corresponding author wrote the manuscript and proofread it. The co-author worked as a data analysis consultant. All authors contributed to the shape of the research, research analysis, and manuscript and agreed to the final version of this manuscript.

■ REFERENCES

[1] Trisunaryanti, W., Larasati, S., Triyono, T., Santoso, N.R., and Paramesti, C., 2020, Selective production of green hydrocarbons from the hydrotreatment of waste cooking oil over Ni- and NiMo- supported on amine-functionalized mesoporous silica, *Bull. Chem. React. Eng. Catal.*, 15 (2), 415–431.

[2] Nanda, S., Rana, R., Hunter, H.N., Fang, Z., Dalai, A.K., and Kozinski, J.A., 2020, Hydrothermal catalytic processing of waste cooking oil for hydrogen-rich syngas production, *Chem. Eng. Sci.*, 195, 935–945.

[3] Yıldız, A., Goldfarb, J.L., and Ceylan, S., 2019, Sustainable hydrocarbon fuels via "one-pot" catalytic deoxygenation of waste cooking oil using inexpensive, unsupported metal oxide catalysts, *Fuel*, 263, 116750.

[4] Nuntang, S., Yousatit, S., Yokoi, T., and Ngamcharussrivichai, C., 2019, Tunable mesoporosity and hydrophobicity of natural rubber/hexagonal mesoporous silica nanocomposites, *Microporous Mesoporous Mater.*, 275, 235–243.

[5] Irzon, R., 2018, Komposisi kimia pasir pantai di selatan Kulon Progo dan implikasi terhadap provenance, *JGSM,* 19 (1), 31–46.

[6] Salamah, S., Trisunaryanti, W., Kartini I., and Purwono, S., 2021, Synthesis and characterization of mesoporous silica from beach sand as silica source, *IOP Conf. Ser.: Mater. Sci. Eng.,* 1053, 012027.

[7] Thahir, R., Wahab, A.W., Nafie, N.L., and Raya, I., 2019, Synthesis of mesoporous silica SBA-15 through surfactant set-up and hydrothermal process, *Rayasan J. Chem.*, 12 (3), 1117–1126.

[8] Salamah, S., Trisunaryanti, W., Kartini, I., and Purwono, S., 2021, Hydrocracking of waste cooking oil into biofuel using mesoporous silica from Parangtritis Beach sand synthesis by sonochemistry, *Silicon*, 14, 3583–3590.

[9] Miyao, T., Sakurabayashi, S., Shen, W., Higashiyama, K., and Watanabe, M., 2015, Preparation and catalytic activity of mesoporous Silica-coated Ni-Alumina base catalyst for selective CO methanation, *Catal. Commun.*, 58, 93–96.

[10] Wijaya, K., Kurniawan, A.H., Saputri D., Trisunaryanti, W., Mirzan, M., Harjani, P.L., and Tjkoalu A.D., 2021, Synthesis of nickel catalyst supported on ZrO_2/SO_4 pillared bentonite and its application for conversion of coconut oil into gasoline via hydrocracking process, *J. Environ. Chem. Eng.*, 9 (4), 105399.

[11] Levenspiel, O., 1999, "Chemical Reaction Engineering," in *Chemical Reaction Engineering*, 3rd Ed., John Wiley & Sons, New York, US, 90–119.

[12] Trisunaryanti, W., Sumbogo, S.D., Mukti, R.R., Kartika, I.A., Hartati, and Triyono, 2021, Performance of low-content Pd and high-content Co, Ni supported on hierarchical activated carbon for the hydrotreatment of *Calophyllum inophyllum* oil (CIO), *React. Kinet., Mech. Catal.*, 134 (1), 259–272.

[13] Wijaya, K., Saputri, W.D., Aziz, I.T.A., Wangsa, Heraldy, E., Hakim, L., Suseno, A., and Utami, M.,

2021, Mesoporous silica preparation using sodium bicarbonate as template and application of the silica for hydrocracking of used waste cooking oil into biofuel, *Silicon*, 14 (4), 1583–1591.

[14] Qiu, S., Zhang, Q., Lv, W., Wang, T., Zhang, Q., and Ma, L., 2017, Simply packaging Ni nanoparticles inside SBA-15 channels by co-impregnation for dry reforming of methane, *RSC Adv.*, 7, 24551–24560.

[15] Komaruzzaman, M.F., Taufik-Yap, Y.H., and Derawi D., 2020, Green diesel production from palm fatty acid distillate over SBA-15 supported nickel/cobalt catalyst, *Biomass Bioenergy*, 134, 105476.

[16] Sudhasree, S., Banu, A.S., Brinda, P., and Kurian, G.A, 2014, Synthesis of nickel nanoparticles by chemical and green route and their comparison in respect to biological effect and toxicity, *Toxicol. Environ. Chem.*, 96 (5), 743–754.

[17] Lin, H.Y., and Chen, Y.W., 2005, Preparation of spherical hexagonal mesoporous silica, *J. Porous Mater.*, 12 (2), 95–105.

[18] Lin S., Shi, L., Ribeiro Carrott, M.M.L., Carrott, P.J.M., Rocha, J., Li, M.R., and Zou, X.D., 2011, Direct synthesis without addition of acid of Al-SBA-15 with controllable porosity and high hydrothermal stability, *Microporous Mesoporous Mater.*, 142 (2-3), 526–534.

[19] Wang, N., Yu, X., Shen, K., Chu, W., and Qian, W., 2013, Synthesis, characterization and catalytic performance of MgO-coated Ni/SBA-15 catalysts for methane dry reforming to syngas and hydrogen, *Int. J. Hydrogen Energy*, 38 (23), 9718–9731.

[20] Amin, A.K., Wijaya, K., and Trisunaryanti, W., 2020, Physico-chemical properties of nickel promoted sulfated zirconia powder prepared using different procedures, *Asian J. Chem.*, 32 (3), 555–560.

[21] Pauly, T.R., Liu, Y., Pinnavaia, T.J., Billinge, S.J.L., and Rieker, T.P., 1999, Textural mesoporosity and the catalytic activity of mesoporous molecular sieves with wormhole framework structures, *J. Am. Chem. Soc.*, 121 (38), 8835–8842.

[22] Sotomayor, F.J., Cychosz, K.A., and Thommes, M., 2018, Characterization of micro/mesoporous materials by physisorption: Concepts and case studies, *Acc. Mater. Surf. Res.*, 3 (2), 34–50.

[23] Coasne, B., 2016, Multiscale adsorption and transport in hierarchical porous materials, *New J. Chem.*, 40 (5), 4078–4094.

[24] Kusumastuti, H., Trisunaryanti, W., Falah, I.I., and Marsuki, M.F., 2018, Synthesis of mesoporous silica-alumina from Lapindo mud as support of Ni and Mo metals catalysts for hydrocracking of pyrolyzed α-cellulose, *Rasayan J. Chem.*, 11 (2), 522–530.

[25] Nugraha, A., and Nandiyanto, A.B.D., 2021, How to read and Interpret GC/MS spectra, *IJOMR*, 1 (2), 171–206.

[26] Li, L., Ding, Z., Li, K., Xu, J., Liu, F., Liu, S., Yu, S., Xie, C., and Ge, X., 2016, Liquid hydrocarbon fuels from catalytic cracking of waste cooking oils using ultrastable zeolite USY as catalyst, *J. Anal. Appl. Pyrolysis*, 117, 268–272.

[27] Trisunaryanti, W., Larasati, S., Bahri, S., Ni'mah, Y.L., Efiyanti, L., Amri, K., Nuryanto, R., and Sumbogo, S.D., 2020, Performance comparison of Ni-Fe loaded on NH_2-functionalized mesoporous silica and beach sand in the hydrotreatment of waste palm cooking oil, *J. Environ. Chem. Eng.*, 8 (6), 104477.

[28] Rodiansono, and Trisunaryanti, W., 2005, Activity test and regeneration of NiMo/Z catalyst for hydrocracking of waste plastic fraction to gasoline fraction, *Indones. J. Chem.*, 5 (3), 261–268.

[29] Chen, R.X., and Wang, W.C., 2019, The production of renewable aviation fuel from waste cooking oil. Part I: Bio-alkane conversion through hydro-processing of oil, *Renewable Energy*, 135, 819–835.